2) The thermal contact conductance increases with time throughout the contact portion of the cycle. For longer contact times, the value of h_c attains a peak value and remains near this value for the remainder of the contact. For the case considered here, this peak value of h_c is comparable to the values of h_c reported for steady-state contacts.

3) The ultimate value of h_c appears to be dependent only on t_c in the cycle if all other experimental parameters are constant. For all cases investigated, the values of h_c follow the same curve until the end of the cycle contact/separation interval is attained. Because of this behavior, the thermal contact conductance is not constant throughout the contact period and h_c should not be considered constant for cycles of short duration.

4) Once a quasisteady-state condition is attained, the temperature distribution at the end of the contact period in the high-thermal-conductivity material appears unaffected by the length of contact or separation. However, the temperature distribution at the end of the separation period is influenced by t_c.

5) In the material with the lower thermal conductivity, t_c influences the temperature distribution at the end of both contact and separation.

6) For the examples considered, T^* approaches within 5% of its quasisteady-state value within a maximum of 40% of the total cycles required to reach the actual steady-state condition.

The basic behavior demonstrated by the aluminum/stainless-steel specimens in periodic contact is essentially the same as that demonstrated in the similar metal contact problem investigated by Moses and Johnson.[7,8] The rapidity of the attainment of the nondimensionalized quasisteady-state temperature distribution, the time dependence of the contact conductance, and the influence of contact time on the temperature distribution during separation are all closely paralleled for periodic contact in similar and dissimilar metallic interfaces.

Acknowledgment

This work was supported by a grant from the Amoco Foundation, Inc. The authors also express their appreciation to J. V. Beck for making his inverse conduction solution available.

References

[1]Dodd, N. C., and Moses, W. M., "Heat Transfer Across Aluminum/Stainless-Steel Surfaces in Periodic Contact," AIAA Paper 88-2646, June 1988.

[2]Howard, J. R., and Sutton, A. E., "An Analogue Study of Heat Transfer Through Periodically Contacting Surfaces," *International Journal of Heat and Mass Transfer,* Vol. 13, Jan. 1970, pp. 173–183.

[3]Mikhailov, M. D., "Quasisteady-State Temperature Distribution in Finite Regions with Periodically Contacting Surfaces," *International Journal of Heat and Mass Transfer,* Vol. 17, Dec. 1974, pp. 1475–1478.

[4]Howard, J. R., and Sutton, A. E., "The Effect of Thermal Contact Resistance on the Heat Transfer Between Periodically Contacting Surfaces," *Journal of Heat Transfer,* Vol. 95, Aug. 1973, pp. 411–412.

[5]Vick, B., and Ozisik, M. N., "Quasisteady-State Temperature Distribution in Periodically Contacting Finite Regions," *Journal of Heat Transfer,* Vol. 103, Nov. 1981, pp. 739–744.

[6]Howard, J. R., "An Experimental Study of Heat Transfer Through Periodically Contacting Surfaces," *International Journal of Heat and Mass Transfer,* Vol. 19, April 1976, pp. 367–372.

[7]Moses, W. M., and Johnson, R. R., "Experimental Study of the Transient Heat Transfer Across Periodically Contacting Surfaces," *Journal of Thermophysics and Heat Transfer,* Vol. 2, No. 1, 1988, pp. 37–42.

[8]Moses, W. M., and Johnson, R. R., "Experimental Results for the Quasisteady Heat Transfer Through Periodically Contacting Surfaces," AIAA Paper 87-1608, June 1987.

[9]Beck, J. V., "Combined Parameter and Function Estimation in Heat Transfer with Application to Contact Conductance," *Journal of Heat Transfer,* Vol. 110, Nov. 1988, pp. 1046–1070.

[10]Barzelay, M. E., Jong, K. N., and Holloway, G. F., "Effect of Pressure on Thermal Conductance of Contact Joints," NACA TN-3295, May 1955.

Numerical Study of Two-Dimensional Freezing in an Annulus

S. S. Sablani,* S. P. Venkateshan,† and V. M. K. Sastri‡
Indian Institute of Technology, Madras, India

Introduction

IN thermal energy storage applications, charging/discharging of energy into/from a phase-change medium (PCM) is usually accomplished by passing a fluid through a tube buried inside the PCM. The phase-change material may be limited to a finite annular space surrounding the tube to keep the charge/discharge time within reasonable limits. An analysis of such a situation, particularly when the PCM is initially either undercooled or superheated, is of practical importance. The charge/discharge time depends on various parameters, such as the annular ratio (annular gap/length of tube), Biot number, Stefan number, and thermophysical properties of the PCM. Because of the finite domain in the PCM, the charge/discharge time will also depend on the location of the front with respect to the boundary; i.e., if the freeze/melt front reaches the outer boundary of the annulus, sensible cooling/heating can also occur. These effects have not been given attention in earlier work reported in the literature.[2,3] The present Note discusses the result of a numerical study of two-dimensional freezing in an annulus of an initially superheated PCM. Numerical results are used to deduce a relation between the nondimensional discharge time and the other parameters referred to earlier.

Analysis

Figure 1 shows a schematic of the horizontal annular geometry considered in the present study. Initially the annular gap is full of a PCM in a liquid state and temperature T_e greater than its fusion temperature T_δ. The discharge of energy is started at time $t=0$ by allowing a coolant to flow inside the tube at an inlet temperature T_i ($<T_e$) with an average velocity U. The thickness of the frozen layer varies along the length of the tube because of the temperature rise of the coolant in the axial direction due to energy transfer to the PCM. Assuming that the convection effects are small in the PCM [annular ratio and (T_e-T_δ) are assumed to be small], the freezing is axisymmetric.

The equation governing the problem on the PCM side (frozen/melt region) is the standard two-dimensional heat equation written in cylindrical coordinates. The energy balance at the interface between the frozen and melt region and on the coolant side are similar to the equations given in Refs. 1 and 3. The only difference is in specifying adiabatic boundary conditions on P, R, and S, as shown in Fig. 1. Nondimensionalization of these equations is done by using the nondimensional variables of Ref. 2. The boundary immobilization method[2-5] is used to solve this conjugate phase-change/convection problem. The solution of the second-order parabolic equation is carried out by using the standard finite-difference method employing an alternating-direction implicit scheme.

Received Sept. 14, 1988; revision received Jan. 26, 1989.

*Research Scholar, Department of Mechanical Engineering.
†Assistant Professor, Regional Sophisticated Instrumentation Center, Department of Mechanical Engineering.
‡Professor, Department of Mechanical Engineering.

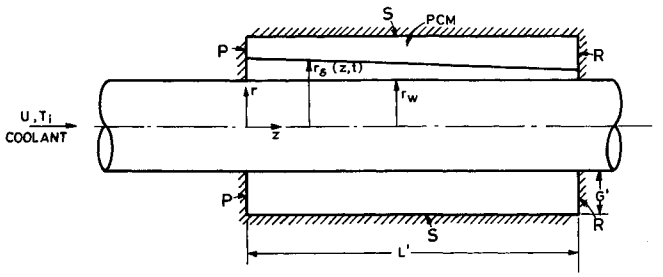

Fig. 1 Schematic diagram of a PCM in an annulus surrounding a coolant-carrying tube. Surfaces *P*, *R*, and *S* are adiabatic. The coolant flow and temperature fields are assumed to be fully developed.

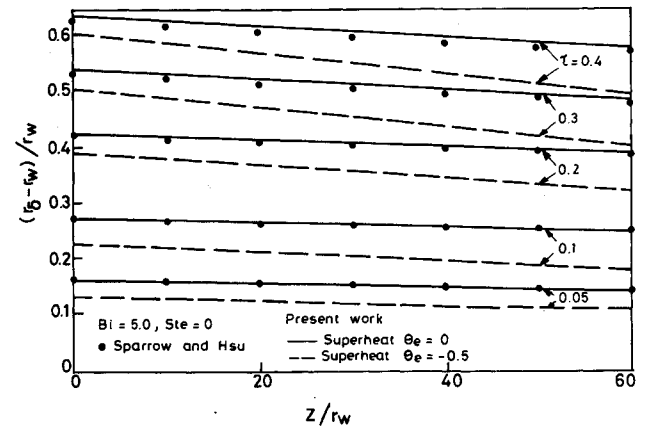

Fig. 2 Variation of freeze front location with axial distance plotted for various times as compared with the calculations of Hsu et al.[2] showing the effect of initial superheat on freezing pattern.

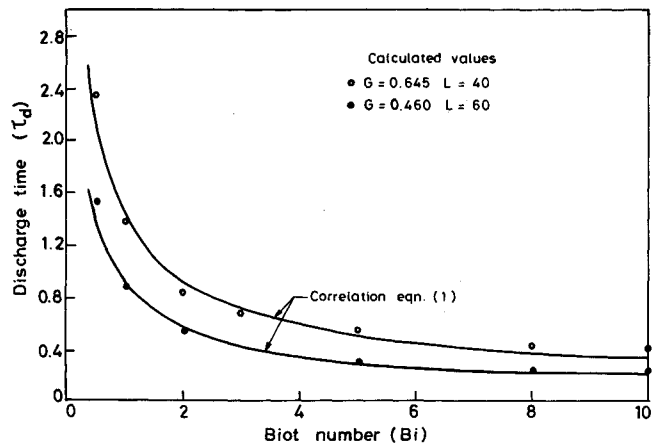

Fig. 3 Variation of discharge time with Biot number for two different geometries having the same volume of PCM. The correlation equation [Eq. (1)] is also plotted.

Keeping the thermal energy storage application in mind, typical values of the nondimensional parameters have been calculated. The Stefan number range is $0 \leq Ste \leq 0.2$ (typical value, 0.1); the Biot number range is $0 \leq Bi \leq 10$; the Stanton number range is $0.001 \leq St \leq 0.006$ (typical value 0.003); and the annular ratio range is $0.0045 \leq (G'/L') \leq 0.03225$. The thermophysical properties of the solid and molten regions are taken to be the same (typical of molten salts). The nondimensional initial temperature of the PCM is kept constant at $\theta_e = (T_e - T_\delta)/T_i - T_\delta) = -0.5$, which represents a mild superheat.

Results and Discussions

The numerical solution of the equations for the typical range of parameters given earlier has been accomplished by making a compromise between accuracy and computational time. Three different step sizes in the spatial direction were used and the final choice was 10 steps each in the radial direction in both the molten and solid regions. The number of steps in the axial direction was relatively large. The axial step size was kept constant at $z/r_w = 1$. In view of the fact that the axial variation of temperature is mild, this gave satisfactory results. The solution is less sensitive to the time-step size[6] and, since the implicit method used here is free from stability constraints, the desired accuracy guided the choice of time-step size. Between $\Delta\tau = 0.01$ and 0.001, there is only a 2% improvement in the calculated values of the discharge time.

The present numerical method was applied to the problem considered in Ref. 2, and the results are in agreement as shown in Fig. 2. Figure 2 also shows the effect of the finite domain and the superheat. Note that the initially superheated liquid PCM takes more time for complete solidification because of the additional sensible heat that has to be removed. The decrease of frozen layer thickness in the axial direction is a consequence of the rise of the coolant temperature as it moves along the tube and the initial superheat in the present case. The two-dimensional effects are more severe in the present case as compared with the no-superheat case. The velocity of the freeze front decreases with time because of the increase of interface area as the freezing proceeds radially outwards. As the freeze front approaches the outer boundary, there is a marginal decrease in the freezing rate because of the presence of the adiabatic surface in the present case. The freeze front reaches the outer boundary in a progressive fashion from entry to exit. During this period, sensible cooling occurs only in the region where the freeze front has already reached the adiabatic surface.

The most important parameter for the present application is the nondimensional discharge time $\tau_d = Ste \cdot Fo$, where the Fourier number is based on thermal diffusivity of the solid PCM, the radius of the tube, and the discharge time—the time taken for the complete solidification of PCM. The Stefan number, apart from its appearance in the definition of τ_d, does not affect the results otherwise. The Biot number plays an important role: the freezing rate increases with the Biot number approaching the isothermal wall condition in the limit $Bi \infty$. As the Biot number decreases, the discharge time increases sharply, with the rate of freezing remaining relatively constant during the entire solidification process.

With the Stefan number kept constant at 0.1, several (65 sets) calculations were performed accounting for the variation of the significant parameters referred to earlier. All of these data can be related by the following correlation (correlation coefficient of 0.998; standard deviation of error is 0.0575):

$$\tau_d = 1.598\, Bi^{-0.639}\, L^{0.153}\, G^{1.533} \qquad (1)$$

where $L = L'/r_w$ and $G = G'/r_w$.

Figure 3 shows the effect of Biot number on discharge time for two different cases by with the same volume of PCM and the same amount of superheat to demonstrate the effect of geometry on discharge time. Note that the smaller annular ratio reduces the discharge time considerably. Figure 3 also shows that numerical results are modeled by Eq. (1) very well.

References

[1]Crank, J., *Free and Moving Boundary Problems,* Claredon, Oxford, 1984, pp. 16–19.

[2]Hsu, C. F., Sparrow, E. M., and Patankar, S. V., "Numerical Solution of Moving Boundary Problems by Boundary Immobilization and a Control-Volume Based Finite Difference Scheme," *International Journal of Heat and Mass Transfer,* Vol. 24, 1981, pp. 1335–1343.

[3]Sparrow, E. M., and Hsu, C. F., "Analysis of Two Dimensional Freezing on the Outside of a Coolant Carrying Tube," *International*

Journal of Heat and Mass Transfer, Vol. 24, Aug. 1981, pp. 1345–1357.

[4]Saitoh, T., "Numerical Methods for Multidimensional Freezing in Arbitrary Domains," *ASME Journal of Heat Transfer,* Vol. 100, May 1978, pp. 294–299.

[5]Duda, J. L., Malone, M. F., Notter, R. H., and Vrentas, J. S., "Analysis of Two Dimensional Diffusion-Controlled Moving Boundary Problems," *International Journal of Heat and Mass Transfer,* Vol. 18, May 1975, pp. 901–910.

[6]Shamsunder, N., and Rooz, E., "Numerical Methods for Moving Boundary Problems," *Handbook of Numerical Heat Transfer,* Wiley, New York, 1988, pp. 747–786.

Parallel-Flow and Counter-Flow Conjugate Convection from a Vertical Insulated Pipe

J. Libera* and D. Poulikakos†
University of Illinois at Chicago, Chicago, Illinois 60680

Nomenclature

A = dimensionless group, Eq. (22)
B = dimensionless group, Eq. (6)
c_{pl} = specific heat of pipe fluid
g = acceleration of gravity
H = length of pipe
h = heat-transfer coefficient
K = permeability of porous material
k = thermal conductivity
Nu = Nusselt number
Pe = Peclet number, Eq. (8)
Pr = Prandtl number
q = heat flux perpendicular to flow direction
R = radius of pipe
r = radial direction, Fig. 1
Ra_κ = Darcy modified Rayleigh number, Eq. (13)
T_1 = mean temperature of the pipe fluid, $2/R_i^2U\int_0^{R_i}u_1t_1r\,dr$
T_2 = temperature of the fluid in the insulation
t_1 = temperature
U = mean velocity of pipe fluid
u = velocity component in the x direction
v = velocity component in the y direction
x = coordinate parallel to flow direction
y = coordinate perpendicular to flow direction
α = thermal diffusivity of pipe fluid
β = coefficient of thermal expansion
λ = Oseen function
ν = kinematic viscosity
ρ = fluid density
θ = dimensionless temperature

Subscripts
c = cold
i = inner surface of pipe
o = outer surface of pipe
w = pipe wall
$*$ = dimensional variable
∞ = reservoir condition far away from the pipe
1 = pipe fluid
2 = reservoir fluid

Received Jan. 5, 1989; revision received Sept. 25, 1989.

*Research Assistant, Department of Mechanical Engineering.
†Associate Professor, Department of Mechanical Engineering.

Introduction

CONJUGATE heat transfer finds numerous applications in thermal engineering. It is because of this reason that conjugate heat transfer has been the main focal point in several investigations over the past few decades. Since convection is a common heat-transfer mode, it is reasonable to expect that it often constitutes one of the two or more interweaving modes (mechanisms) in conjugate heat-transfer applications. For example, Poulikakos[1] studied theoretically the problem of natural convection along a vertical conductive wall coupled with film condensation on the other side of this wall. He determined the parametric domain over which the two coupled phenomena (natural convection and condensation) seriously affect each other as well as the overall heat transfer through the wall. In a related study, Poulikakos and Sura[2] investigated the interaction between condensation inside a vertical layer of insulation and natural convection at the surface of the insulation. Faghri and Sparrow[3] examined theoretically the coupling of condensation on a pipe and forced convection of a fluid inside the pipe. Also theoretical is the work of Bejan and Anderson,[4,5] who investigated the problem of natural convection along the impermeable interface of two fluid reservoirs[4] and a porous and fluid reservoir,[5] respectively. In the work of Bejan and Anderson,[4,5] the coupling was between two different counter-flowing boundary layers.

The present Note investigates the problem of interaction (coupling) of forced convection inside a vertical pipe and natural convection outside the pipe, where the pipe is surrounded by permeable insulation. This analysis finds applications in the design of insulation jackets for pipes, where the insulation can be modeled as an isotropic porous medium. It also provides the means for calculating heat-transfer gains or losses from a buried vertical pipe. Both the cases of counter flow and parallel flow are considered. Clearly, the heat transfer through the pipe wall is a direct result of the interaction between the forced convection inside the pipe and the natural convection outside the pipe.

Formulation and Analysis

Consider the system shown in Fig. 1a. A warm fluid is flowing inside a vertical conductive pipe opposite to the direction of gravity. The pipe is surrounded by a porous material saturated with a colder fluid, which is assumed to be in thermal equilibrium with the porous matrix. The heating effect of the forced convection in the pipe is responsible for the establishment of temperature gradients inside the porous reservoir. These gradients in turn trigger a natural convection flow in the direction opposite to gravity. Clearly, the temperature of the fluid in the pipe varies along the flow passage as does the wall temperature and the temperature difference across the natural convection current, which is assumed to be of the boundary-layer type. Therefore, the local and overall heat transfer from the fluid in the pipe to the porous material depends on the preceding conjugate heat-transfer mechanisms (natural convection and forced convection). Figure 1b pertains to the same phenomenon just explained with the difference that the fluid in the pipe and the fluid in the reservoir are flowing in the opposite direction (counterflow configuration).

To formulate the problem mathematically, we will focus first on the forced-convection side and next on the natural-convection side of the parallel-flow configuration in Fig. 1a.

Forced Convection Inside the Pipe

At any axial position the heat-transfer rate from the forced-convection side through the pipe wall to the natural-convection side is

$$dq = \frac{2\pi k_w}{\ell n(R_i/R_o)}(T_{w_i} - T_{w_o})\,dx^* \tag{1}$$

The heat-transfer rate convected to the inner surface of the pipe over a length dx^* is

$$dq = 2\pi R_i h_i (T_1 - T_{w_i})\,dx^* \tag{2}$$